PROCEEDINGS OF SCIENCE

Energy-dependent variability in blazars SSC simulations

David Sanchez
Laboratoire Leprince-Ringuet, CNRS/IN2P3,
Ecole Polytechnique,
91128 Palaiseau, France
E-mail: dsanchez@llr.in2p3.fr

Berrie Giebels
Laboratoire Leprince-Ringuet, CNRS/IN2P3,
Ecole Polytechnique,
91128 Palaiseau, France
E-mail: berrie@in2p3.fr

Guillaume Dubus
Laboratoire d'Astrophysique de Grenoble, CNRS,
Université Joseph Fourier, BP 53,
38041 Grenoble, France
E-mail: Guillaume.Dubus@obs.ujf-grenoble.fr

The light curves of blazars have been studied from radio wavelengths up to very high energy gamma-rays, and their statistical properties seem to be often compatible with a red noise process, where variability power decreases with increasing frequency. An increase of light curve variance with energy has been reported by some authors. In order to reproduce the statistical properties of a blazar light curve, and also the energy dependence of the normalised variance F_{var}, we study the injection of a time-dependent electron distribution in a spherical emission region. A simple SSC model is then used to derive the time-dependent electromagnetic spectrum, which allows us to derive the resulting energy-dependent variance in the range of a few eV up to X-rays. We show that this model can reproduce the increase of the variance with energy by just taking emission processes into account. We also make some predictions for the GLAST energy range based on the results of a multiwavelength campaign on Mkn 421.

Workshop on Blazar Variability across the Electromagnetic Spectrum
April 22-25 2008
Palaiseau, France

PoS(BLAZARS2008)034

1. Introduction

The innermost regions of active galactic nuclei, where the largest part of their luminosity is emitted, can be probed through observations of their flux variability at different wavelengths. Physical processes in their central engines and jets are the main candidates for the origin of the observed variability. Measurements of correlated variability, spectral variations and time lags across broadband observations allow modelling of particle distributions and radiative processes, and to probe the acceleration mechanisms that are involved.

Variability can be characterized using a wide variety of estimators, depending mostly on the quality of the observed time series. With well-sampled light curves it becomes possible to study the variability through the power spectrum density (PSD), obtained by a direct Fourier transform of the light curve. Generally, these PSDs exhibit a featureless continuum best described by a power law with an index of ≈ 2 or less, indicating that power increases with decreasing frequency (see e.g. [6] [7]). In this study we aim to understand the energy-dependent variability observed in Mkn421 [1] and PKS2155-304 [2] and notably the fact that normalized variances from the optical to the X-rays appear to also increase as a power law of the observed energy (while the light curves are not necessary correlated).

In order to reproduce such an chromatic effect we study the electromagnetic output of an electron distribution injected according to a red noise time profile, using a synchrotron-self Compton (SSC) scenario. Section 2 describes the SSC model and the method to generate injections with a red noise profile. In section 3 , we compare the results to the data obtained during a multiwavelength (MWL) campaign on Mkn 421 in 2001 [1] and give the result for a single injection. We then discuss the energy dependence of the variance between a few eV and 10^4 eV, and make a prediction for the GLAST telescope in a higher energy band than the observations considered here.

2. SSC model and red noise generation

In this section, we describe our SSC model and the method used to generate time series with a red noise profile.

2.1 Description of the SSC model

The spectral energy distribution (SED) of blazars shows two broad peaks in $\nu F_(\nu)$ representation. It is well established that the low energy peak is due to synchrotron emission of relativistic electrons, and that inverse Compton (IC) emission of electrons in a soft photon field is probably the cause of the high energy peak. The origin of the seed photons is unknown, but are usually considered as being either the synchrotron photons themselves (synchrotron self-Compton, SSC hereafter) or photons external to the emission region (external Compton, EC). High-frequency peaked BL Lac objects, such as Mkn 421, are usually modelled in the SSC scenario. We use a simple one-zone SSC model, assuming an homogeneous sphere of radius R to be the emitting region in which the magnetic field B is constant. Electrons are injected in the sphere and lose energy by synchrotron and inverse Compton radiation.

The used SSC model is derived from [4]. The time-dependent electron distribution evolution is given by the diffusion equation:

$$\frac{\partial N_e}{\partial t} = \frac{\partial}{\partial}[(\dot{\gamma}_s + \dot{\gamma}_c)N_e(\gamma,t)] + Q(\gamma,t) - \frac{N_e(\gamma,t)}{t_{esc}} \tag{2.1}$$

and the injection term is a maxwellian distribution:

$$Q(t,\gamma) = K\gamma^2 \exp(-2\gamma/\gamma_b(t)) \tag{2.2}$$

where $\gamma_b(t)$ is time-dependent (as in [1]). Equation 2.1 is a Fokker-Planck equation without diffusive term. We use a slightly modifed Chang and Cooper scheme to discretize 2.1 in time (with step dt) and energy.

As in [1], we chose our physical parameters to be $B = 0.2$ G, $R = 2\times10^{15}$ cm and bulk Lorentz factor $\Gamma = 40$.

First of all, we define the quiescent state to be the steady state with our set of parameters. In addition of B,R and Γ, we take $\gamma_b = 5.3\times10^3$ and $K = 7.9\times10^{18}\mathrm{cm}^{-3}$ for the injection parameters to describe the quiescent state and to be the minimal values during the simulation. Electrons are continuously injected according to the maxwellian distribution with a constant value of γ_b until we reach the steady state.

At this point, electrons begin to be injected following a time-dependent distribution with time scale Δt_{inj}. γ_b is given by the simulated time series and K is kept constant. This time scale is expected to be bigger than the light travel time through the sphere (R/c). We take $\Delta t_{inj} = 3R/c$ and $dt = 0.2R/c$. For a typical simulation, we made 512 time steps (Δt_{inj}), which corresponds to 1536 $\Gamma^{-1}R/c = 29.6$ days in the observer's rest frame.

2.2 Red noise generation

The time-dependent electron injection will depend on the acceleration mechanism. Here we want to test the chromatic effect of an injection with parameters varying according to a stochastic process, generated from a red noise spectrum and independant of the emission process as described by [5].

We generate a red noise time series $f(t)$ with a power spectrum density $\propto w^{-\beta}$ following the method of Timmer and Koening (see [3]). The frequency w is in the range $[9.8\times10^{-9}, 1/\Delta t_{inj} = 2.5\times10^{-5}]$ Hz and $\beta = 2$.

First, we calculate a PSD $s(w) = w^{-\beta}$. In the Fourier space, we draw two gaussian distribued random numbers such as $x, y = N(1,0)$; the Fourier transform of the time series is:

$$\tilde{f}(w) = \sqrt{\frac{1}{2}s(w)(x+iy)} \tag{2.3}$$

The resulting periodogram is $|f|^2 \propto s(w)$. The time series is obtained by an inverse Fourier transform. In fact, we simulate a light curve with 5120 points and keep only the first 512 points. This ensures that the Fourier modes with frequency $w \leq 1/\Delta t_{inj}$ contribute to the time series in the real space. The variance of the time series can be adjusted by adding a factor in equation 2.3. Figure 2.2 shows a typical time series and its PSD. The latter is consistent with the theoretical curve in red.

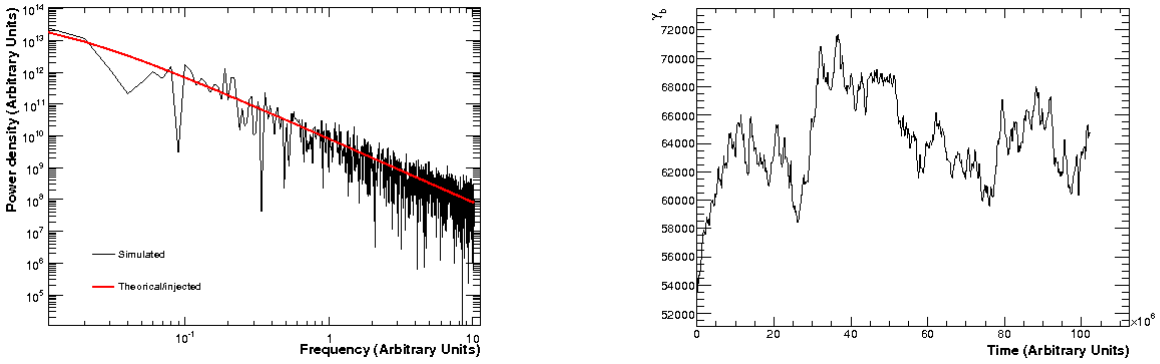

Figure 1: Example of an injected time series computed with the method described in [3]. Left panel: power spectrum density $|f|^2$ as a function of the frequency (black), where the theoretical PSD is the red line. Right panel: resulting time series.

3. Results

We define the normalized variance as :

$$\mathrm{F_{var}} = \sqrt{\frac{S^2}{\bar{x}^2}} \tag{3.1}$$

where S^2 is the variance of the time series and $\bar{x}$ is its average. Figure 2 shows $\mathrm{F_{var}} = F(E)$ for one realisation. The IC emission dominates above a few MeV, decreasing the variability.

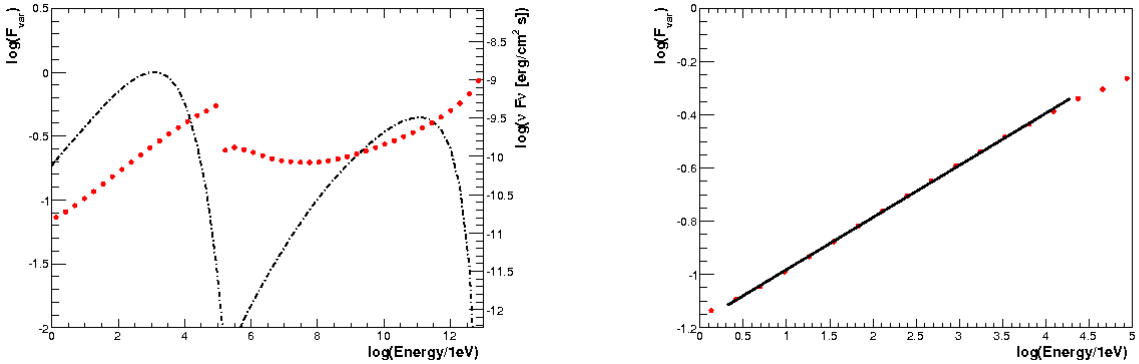

Figure 2: Left panel: $\mathrm{F_{var}}$ versus energy between 1 eV and 10^{14} eV. The dashed line is the spectral energy distribution at the beginning of the simulation. Right panel: zoom in the range 1 eV, 10^5 eV. The black line is the result of a power law fit over the range, yielding an index of ≈ 0.19.

Figure 3 is the PSD of the resulting light curve. We summed the flux at all wavelengths and made a direct Fourier transform. The PSD exhibits a featureless, decreasing profile, evidence of the injected red noise process. Our simulations find $\propto E^{0.19}$ in rather good agreement with the energy-dependent variance $\propto E^{0.25}$ found by [1] in the range $2\ \mathrm{eV} < E < 2 \times 10^4$ eV.

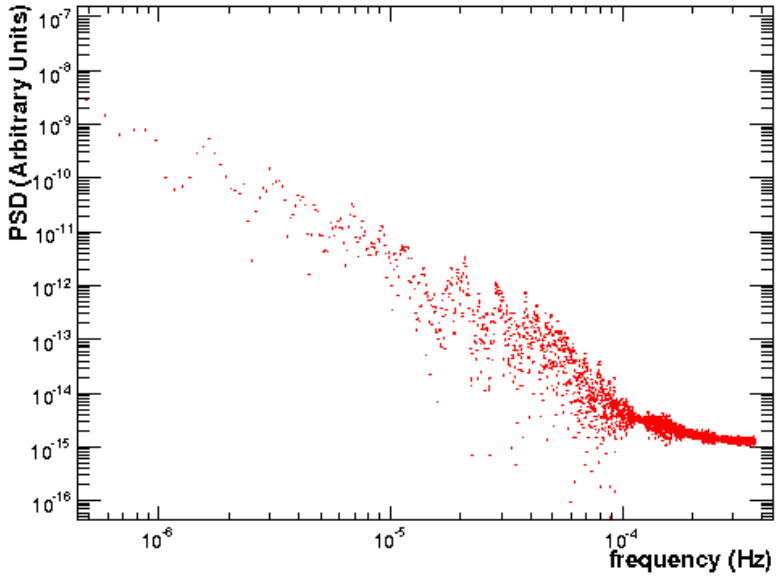

Figure 3: PSD of the light curve obtained by summing flux at all wavelengths.

4. The Gamma-ray Large Area Space Telescope GLAST

Associated with atmospheric Čerenkov telescopes (IACT), GLAST will allow variability studies of AGNs between 30 MeV and 200 GeV. With its large area and good sensitivity, GLAST will be able to see variability on time scales of the order of the day. In figure 4, we focus on the GLAST and IACT energy range, where the IC emission dominate. We predict a lower variability in the GLAST range (30 % on average) compared to the TeV energy range (65 %) for Mkn 421, because cooling timescales are longer for electrons radiating at this energies.

5. Conclusion

With a simple SSC model and electron distributions injected according to a red noise process, we were able to produce a power-law dependency of the normalized variance, with an exponent slightly below those observed. We plan to study possible constraints of e.g. the magnetic field by understanding the energy-dependent variability, as well as the link between the injection function and the observed temporal properties.

References

[1] B. Khelifi B. Giebels, G. Dubus. Unveiling the X-ray/TeV engine in Mkn 421. *A&A*, 462:29–41, 2007.

[2] L. Maraschi et al. A full orbit XMM-Newton observation of PKS 2155-304. *arXiv:astro-ph*, 0202418v1, 2002.

[3] Timmer J. and Koenig. On generating power law noise. *A&A*, 300:707–710, 1995.

[4] J.Kataoka. *X-ray Study of Rapid Variability in TeV Blazars and the Implications on Particle Acceleration in Jets*. PhD thesis, ISAS, 2000.

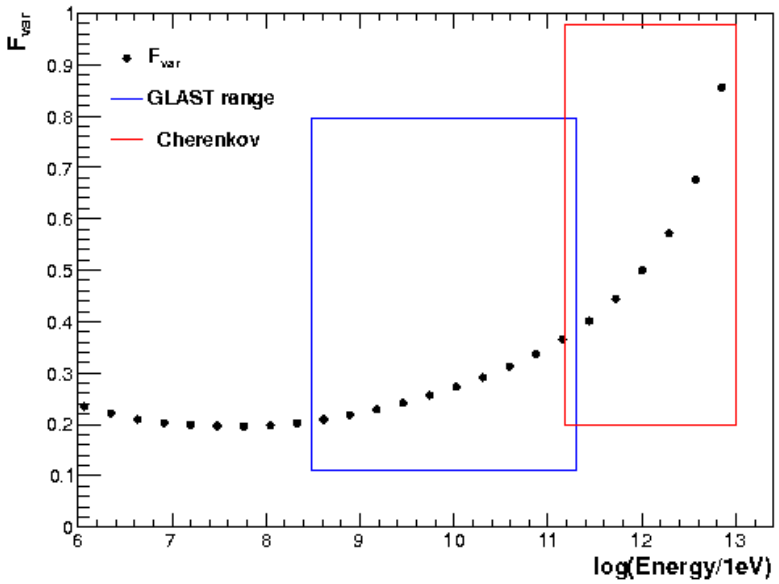

Figure 4: F_{var} as a function of energy between 1 MeV and 10 TeV. The blue box is the GLAST energy range and the red one is the IACT energy range.

[5] I McHardy. Characterising X-Ray Variability in Blazars. *these Proceedings*, 2008.

[6] R. S. Warwick S. Vaughan, R. Edelson and P. Uttley. On characterising the variability properties of X-ray light curves from active galaxies. *Mon. Not. Roy. Astron. Soc.*, 345:1271, 2003.

[7] Y. H. Zhang, A. Celotti, A. Treves, L. Chiappetti, G. Ghisellini, L. Maraschi, E. Pian, G. Tagliaferri, F. Tavecchio, and C. M. Urry. Rapid X-Ray Variability of the BL Lacertae Object PKS 2155-304. *ApJ*, 527:719–732, 1999.